High performance NO_2 sensor using MoS_2 nanowires network

Rahul Kumar, Neeraj Goel, and Mahesh Kumar

Citation: Appl. Phys. Lett. **112**, 053502 (2018);
View online: https://doi.org/10.1063/1.5019296
View Table of Contents: http://aip.scitation.org/toc/apl/112/5
Published by the American Institute of Physics

High performance NO_2 sensor using MoS_2 nanowires network

Rahul Kumar, Neeraj Goel, and Mahesh Kumar[a)]
Department of Electrical Engineering, Indian Institute of Technology Jodhpur, Jodhpur 342011, India

(Received 13 December 2017; accepted 17 January 2018; published online 31 January 2018)

We report on a high-performance NO_2 sensor based on a one dimensional MoS_2 nanowire (NW) network. The MoS_2 NW network was synthesized using chemical transport reaction through controlled turbulent vapor flow. The crystal structure and surface morphology of MoS_2 NWs were confirmed by X-ray diffraction, Raman spectroscopy, X-ray photoelectron spectroscopy, and scanning electron microscopy. Further, the sensing behavior of the nanowires was investigated at different temperatures for various concentrations of NO_2 and the sensor exhibited about 2-fold enhanced sensitivity with a low detection limit of 4.6 ppb for NO_2 at 60 °C compared to sensitivity at room temperature. Moreover, it showed a fast response (16 s) with complete recovery (172 s) at 60 °C, while sensitivity of the device was decreased at 120 °C. The efficient sensing with reliable selectivity toward NO_2 of the nanowires is attributed to a combination of abundant active edge sites along with a large surface area and tuning of the potential barrier at the intersections of nanowires during adsorption/desorption of gas molecules. *Published by AIP Publishing*. https://doi.org/10.1063/1.5019296

The ever increasing industrialization has resulted in raising the concentration of toxic gases in the environment at an alarming rate. Among these gases, NO_2 is one of the most common air pollutants which is hazardous for human health even at a level greater than 1 ppm.[1] Therefore, its detection is an absolute necessity for a healthy ambience. In recent years, two dimensional (2D) material based gas sensors have received considerable attention for monitoring NO_2 due to their large surface to volume ratio, uncomplicated gas sensing mechanism, and outstanding electronic properties.

2D MoS_2 has been greatly admired for its potential applications in gas sensing because of its distinctive physical, chemical, and electronic properties.[2–5] MoS_2 is a layered material consisting of hexagonally packed Mo atoms in a layer sandwiched between two sulfur atom layers (S-Mo-S) and each layer held together by van der Waals force.[6] The MoS_2 nanostructure analogous to the graphene nanosheet has opened new avenues to synthesize nanotubes, nanowires (NWs), and vertically or horizontally aligned MoS_2 flakes using the simple fabrication process for desired device applications.[7–9] For sensing applications, surface topology of the MoS_2 showed the crucial role in enhancing the sensing performance by providing more reactive sites. For instance, vertically aligned MoS_2 showed about a five times higher response to NO_2 compared to horizontally aligned MoS_2.[4] The sensitive edges of the atomically scaled surface structure of MoS_2 provide more reactive sites for gas absorption. Therefore, even the minute traces of NO_2 can be detected by using the nanostructures with exposed edges. However, the slow response and recovery kinetics obstruct the use of these nanostructures for practical gas sensing applications. In addition, most fascinating 2D graphene has attracted much attention in chemical sensing in recent years, and Wang *et al.* reported a review on the graphene based sensor for toxic and combustible gases as well as vapor of volatile organic compounds.[10] On the other hand, Kadhim *et al.* demonstrated a room temperature (RT) efficient hydrogen gas sensor with a power consumption of 65 μW using Pd finger electrode contact on a glycerine added nanocrystalline SnO_2 film.[11] However, in recent years, one-dimensional (1D) nanostructures such as metal oxide nanowires, carbon nanotubes, and silicon nanowires have facilitated both the high response to analytes and the fast response as well as recovery kinetics.[12–14] Recently, Saaedi and Yousefi reported that Na and K doped ZnO nanorods revealed high sensitivity with less response/recovery time to ethanol at its operating temperatures of 280 and 300 °C, respectively, as compared to undoped ZnO nanorods.[12] However, single nanowire based devices are fabricated through expensive as well as time-consuming sophisticated processes such as electron-beam lithography. Moreover, the resistance of the single nanowire based device can be varied due to the different diameter of the distinct nanowire, while the averaging effect in the nanowire network facilitates a simple fabrication procedure with reproducible results. In this context, we can conclude that the one dimensional nanowire (NW) network could be highly useful for efficient sensing.

In this work, we synthesized MoS_2 nanowires under the kinetics conditions by the conventional chemical vapor deposition (CVD) process. As a proof of concept application, we investigated the sensing behavior of MoS_2 NWs to different ppm concentrations of NO_2 at room temperature, 60 °C, and 120 °C.

Large area MoS_2 NWs were grown using MoO_3 and sulfur as precursors by the conventional CVD technique. The substrate was placed in an inclined position near (2 cm) the downstream on one side of the alumina boat which has 0.03 g of MoO_3 while covering the other side of the boat. This typical arrangement was made for a turbulent flow regime, resulting in the formation of MoS_2 NWs. Due to turbulent gas flow, the MoS_2 NWs were grown under the kinetic conditions and the conventional thermodynamics do not play any significant role. The temperatures of the regions containing MoO_3 and sulfur were raised up to 900 °C and

a)Author to whom correspondence should be addressed: mkumar@iitj.ac.in

200 °C, respectively, and the Ar flow was kept at 95 sccm at atmospheric pressure for an hour. The MoS_2 structure and surface morphology were characterized by Raman spectroscopy (Renishaw single monochromator equipped with a CCD), X-Ray diffractometry (Bruker D8 advanced diffractometer), X-ray photoelectron spectroscopic (Scienta Omicron, Germany) measurement using a monochromatized Al Kα (1486.7 eV) radiation source, and SEM (EVO 18 Zeiss with an accelerating voltage of 20 kV). The sensor's temperature was raised by using an external heating filament, and a change in relative resistance of the device at 1.5 V in the gas environment was measured using a Keithley 4200 semiconductor characterization system.

The MoS_2 NWs grown under the kinetic conditions through turbulent flow using CVD have also been revealed in the previous reports.[15,16] However, density of nanowires on the large substrate was less in all reports. Here, high density nanowires (with the diameter from nanometres to several micrometres) as well as vertical oriented triangular shaped flakes of MoS_2 formed the 3D network, as shown in Figs. 1(a) and 1(b).

To examine the alignment and confirmation of CVD grown MoS_2 NWs on the insulating substrate, we used X-ray diffraction (XRD) assessment. The XRD pattern showed the different peaks corresponding to the crystal plane of 2H-MoS_2 (MoS_2 JCPDS # 37–1492) with another peak at 33° corresponding to the Si substrate [Fig. 1(c)]. The high peak intensity of the (100) plane indicates exposed edge sites of MoS_2 compared to the low peak intensity of the (200) plane (exposed basal plane).[4,17] Further, the alignment and crystallinity of the MoS_2 nanowire were confirmed by Raman spectroscopy. Two Raman modes E^1_{2g} (in-plane vibration) and A_{1g} (out-of-plane vibration) are located at ~380 and ~405 cm^{-1}, respectively [Fig. 1(d)]. The intensity ratio E^1_{2g}/A_{1g} of 0.39 indicates exposed abundant edge sites compared to the basal plane and is in good agreement with the previous report on exposed edges of 2H-MoS_2.[4,18] In addition, the MoS_2 NW network was also characterized using XPS to confirm and determine the elemental and chemical composition. From the survey spectrum [Fig. 2(c)], two additional distinctive peaks corresponding to C 1s and O 1s with Mo 3d and S 2p are observed, which is a signature of the presence of oxygen and carbon on the active exposed edge sites of nanowires.[19] Further, deconvolution of the high resolution peaks of Mo 3d and S 2p showed that the doublet at 229.1 and 232.2 eV corresponds to Mo $3d_{5/2}$ and Mo $3d_{3/2}$ and another doublet at 161.9 and 163.0 eV is related to S 2 $p_{3/2}$ and S 2 $p_{1/2}$, respectively [Figs. 2(a) and 2(b)]. Moreover, one peak corresponding to S 2s (an indication of multiple chemical states of sulfur) is located at 226.3 eV. These values and shapes of the peaks are consistent with CVD grown 2H-MoS_2.[20]

To assess the potential of MoS_2 NWs in gas sensing, we fabricated the chemiresistor after depositing two Au/Cr (200/5 nm) electrodes with 100 μm distance between both using shadow mask [schematic of the sensor, Fig. 2(d)]. Afterward, we investigated the sensing behavior of the device for 1, 2, 3, and 5 ppm NO_2 at room temperature, 60 °C, and 120 °C. The dynamic relative response [$\Delta R/R_0 = (R_0 - R_g)/R_0$, where R_g = is the resistance of the device in the gas environment and R_0 = is the initial resistance of the device in vacuum] of the device to varying NO_2 concentrations at room temperature is shown in Fig. 3(a). It was observed that the negative relative response of the device increased with the increasing concentration of NO_2. NO_2, being an oxidizing gas, extracts the electron from MoS_2 because of having an unpair electron. As MoS_2 is an n-type semiconductor, resistance of the device was increased upon exposure to NO_2. However, the device showed incomplete recovery at room temperature due to the strong binding between NO_2 and the reactive sites of MoS_2. Further, to determine the optimum operating temperature of the device for practical sensing, we investigated the sensing

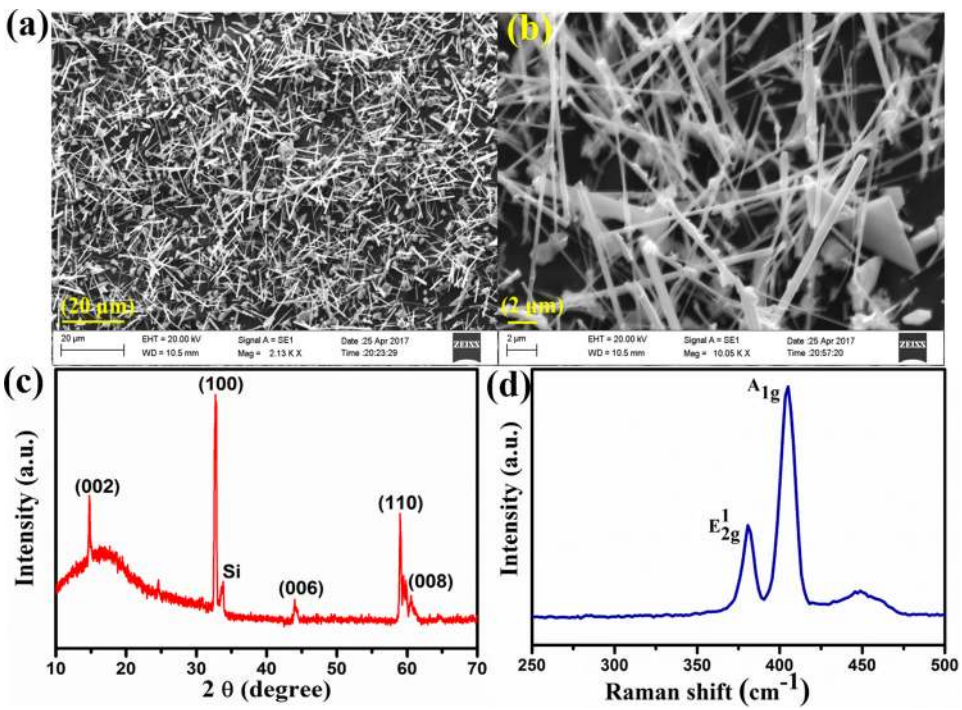

FIG. 1. (a) SEM image of the MoS_2 nanowire (NW) network, (b) a magnified view of the nanowire network, (c) X-ray diffraction (XRD) patterns, and (d) Raman spectrum of the MoS_2 NW network.

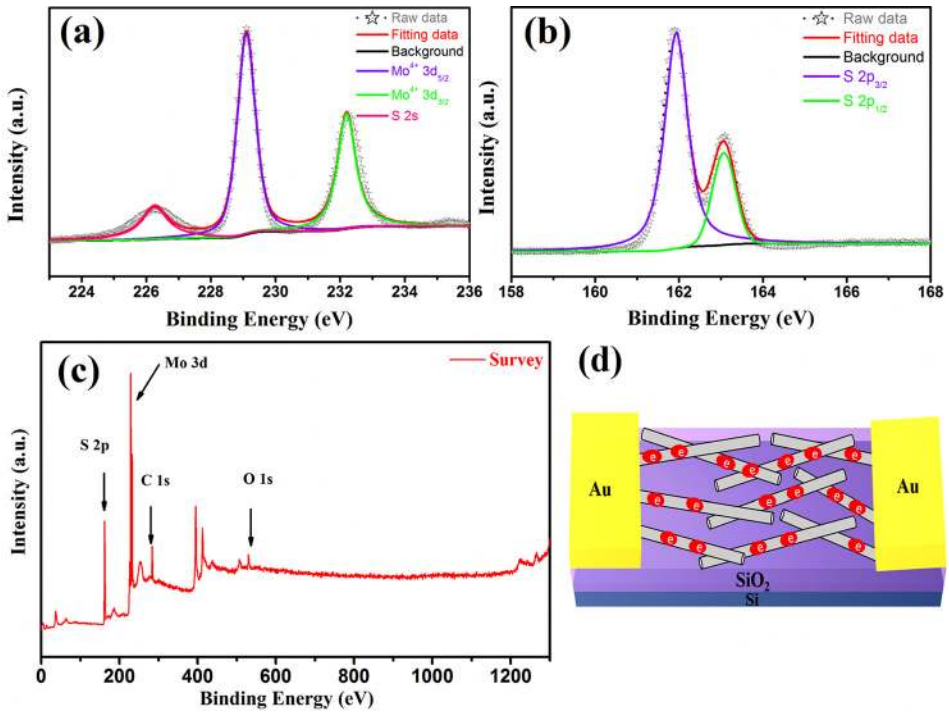

FIG. 2. (a) High-resolution Mo 3d spectra and (b) high-resolution S 2p spectra of the MoS_2 NW network. (c) XPS survey spectra indicate the presence of few oxygen and carbon on the MoS_2 nanowire. (d) Schematic illustration of the sensor.

behavior of the device at 60 °C and 120 °C. Interestingly, it was found that the device exhibited complete recovery to NO_2 at 60 °C, as shown in Fig. 3(b). Thermal energy at 60 °C was sufficient to desorb the gas molecules from the surface of the sensing layer. On the other hand, it was noticed that desorption of gas molecules was dominating over the adsorption at 120 °C, because NO_2 interaction reaction with MoS_2 is exothermic.[21] As a result, at 120 °C temperature, the device was able to recover its baseline (initial resistance) but deteriorating its response to NO_2 [Fig. 3(c)]. Similar behavior was also seen in previous reports of 2D material based gas sensors.[2,21] Thus,

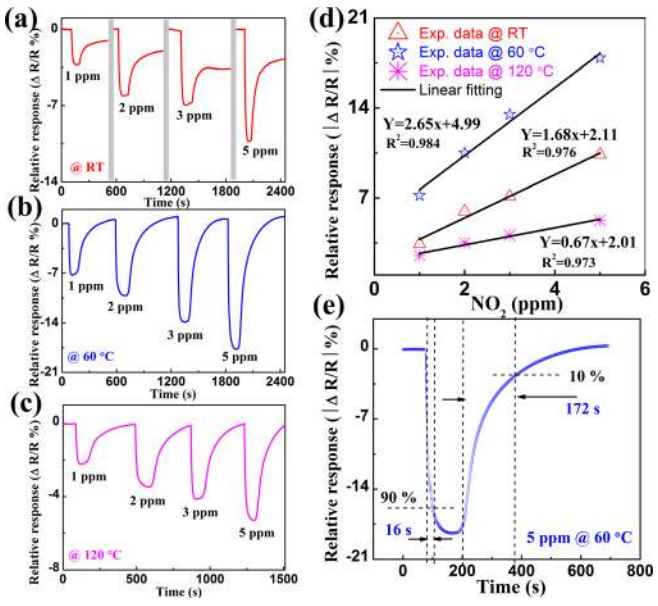

FIG. 3. Transient response of the sensor: (a) at room temperature (RT), (b) at 60 °C, and (c) at 120 °C. (d) Relative response vs NO_2 concentration graph, and here, R^2 shows the quality of curve fitting. (e) Calculation of response and recovery time for 5 ppm of NO_2 at the optimum temperature (60 °C) of the sensor.

it is clearly observed from Fig. 3(d) that the relative response in the range of 7.2–18.1% to NO_2 with the concentration ranging from 1 to 5 ppm at 60 °C is superior to responses at room temperature and 120 °C. In Fig. 3(d), the linear curve fitting of the experimental data of the sensor indicates that a higher slope was achieved at 60 °C which confirms a rapid increase in the response compared to the response at room temperature and 120 °C. However, due to our experimental setup' constraints, we cannot measure the response below 1 ppm concentration. So, we calculated the lowest detection limit (LDL) of the sensor theoretically from experimental data according to the IUPAC definition[22] as $LDL_{ppm} = 3\frac{rms_{noise}}{slope}$, where slope is the slope of linear fitting data from the relative response vs concentration (ppm). For calculation of the rms_{noise} value, we took ten points at baseline of the sensor and fit the fifth order polynomial equation. Subsequently, rms_{noise} was calculated as $rms_{noise} = \sqrt{\frac{(Ri-R)^2}{N}}$, where N is the number of points, R_i are the experimental data points, and R is the value calculated from the fifth order polynomial fitting. The noise and slope values of the sensor are 0.00408 and 2.65 ppm^{-1} (response slope of the fitting line), respectively. So, the LDL value of the sensor for NO_2 was estimated to be about 4.6 ppb.

To gain insight into response and recovery kinetics of the MoS_2 NWs, we calculated the response time of 16 s and recovery time of 172 s to 5 ppm NO_2 at device' optimum operating temperature [Fig. 3(e)]. Here, response and recovery time were calculated based on the time required to reach 90% and 10% of the maximum value after loading and deloading the gas from the sensing chamber, respectively.

In order to understand the selective nature of MoS_2 NWs, sensing behavior of the device was investigated for 5 ppm of NO_2 and 100 ppm of other interfering gases including H_2S, CO_2, CH_4, and H_2 at optimum operating temperature (60 °C) of the sensor (resistance vs time graph, Fig. S1,

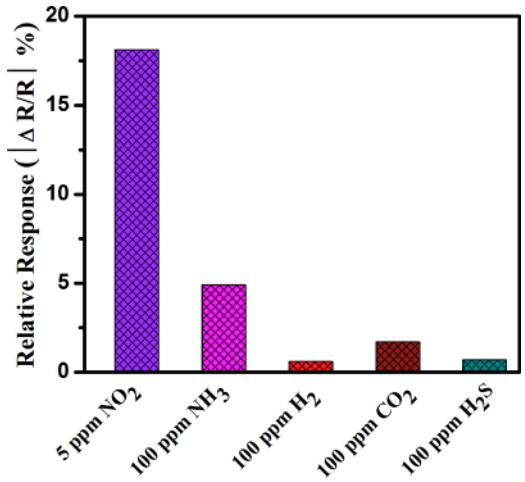

FIG. 4. Relative response of various gases at the optimum temperature (60 °C) of the sensor.

supplementary material). Despite the very low presence of NO_2 in the interfering environment, the device showed a higher relative response to NO_2 against other aforementioned gases (Fig. 4). The reliable selectivity of the sensor is attributed to the high adsorption energy of NO_2 on the exposed edge sites of the MoS_2 compared to other earlier mentioned gases.[23,24]

Here, the gas sensing mechanism of the 2D MoS_2 NW network is attributed to the changed carrier concentration of MoS_2 due to physisorption or chemisorption, or both, of the gas molecules. A variation in carrier density depends mainly on the behavior (oxidizing or reducing) of gas as well as active site density on the surface of MoS_2. At room temperature, a large number of reactive sites are occupied with oxygen and humidity, which extract electrons after reacting rapidly with the exposed sites [Mo edge (10 $\bar{1}$ 0) and S edge ($\bar{1}$ 010)] of the MoS_2 NWs.[25,26] Moreover, oxygen was chemisorbed on the sulfur vacancy because high crystalline MoS_2 NWs have high vacancy density than low crystalline MoS_2.[27] Thereby, the electron concentration was decreased and the depletion region was increased at the surface of nanowires as shown in Fig. 5(a). So, on exposure to NO_2, a less number of molecules was absorbed on the nanowire network due to the already presence of oxygen and humidity on the surface, leading to the weak response to NO_2 at room temperature [Fig. 5(a)]. Further, annealing the device at 60 °C in a vacuum, oxygen molecules and humidity were desorbed from the surface of MoS_2 [Fig. 5(b)]. Consequently, the availability of active edge sites and electron concentration in nanowires were enhanced, resulting in the extraction of more number of electrons by NO_2 molecules. So, the high response of the device at 60 °C is attributed to abundant edge sites and defects along with a large surface to volume ratio. To validate this, we measure the I-V characteristic of the device at room temperature and 60 °C in a vacuum and it was found that conduction was less at room temperature (Fig. S2, supplementary material). In addition, modulation of potential barriers at the intersections of the nanowires during adsorption/desorption of gas molecules also assisted in enhancing the sensitivity of the device [Fig. 5(c)].

On the other hand, response and recovery kinetics of the device are superior to other MoS_2 gas sensors (see supplementary material, Table S1). Relatively quick adsorption and desorption of gas molecules from the MoS_2 NWs are attributed to high conductivity as well as rapid interaction of gas molecules with exposed edge sites of nanowires. The high conductivity of the MoS_2 nanowire can be elucidated in part by exposed coordinatively unsaturated Mo atoms (the Mo d orbital originates from the conducting state above the Fermi level) and sulfur vacancies (i.e., Mo cluster) in the MoS_2 NW structure because mainly low Miller index edges are perfect to localize the metallic states.[9,28,29] Moreover, nanowires helped to diffuse the gas molecules rapidly and efficiently in the nanowire network.[11]

In conclusion, we have developed a highly efficient chemiresistor based on a MoS_2 NW network with high selectivity toward NO_2 against various other toxic and combustible gases. The MoS_2 NW network was synthesized through controlled vapor flow using the CVD process. The device exhibited considerable sensitivity (18.1%) and fast response/recovery (16/172 s) to 5 ppm NO_2; moreover, it can detect down to 4.6 ppb. Thus, the 2D MoS_2 NW based sensor is a perfect candidate for air quality monitoring and industrial process control applications for fast and reliable detection of NO_2.

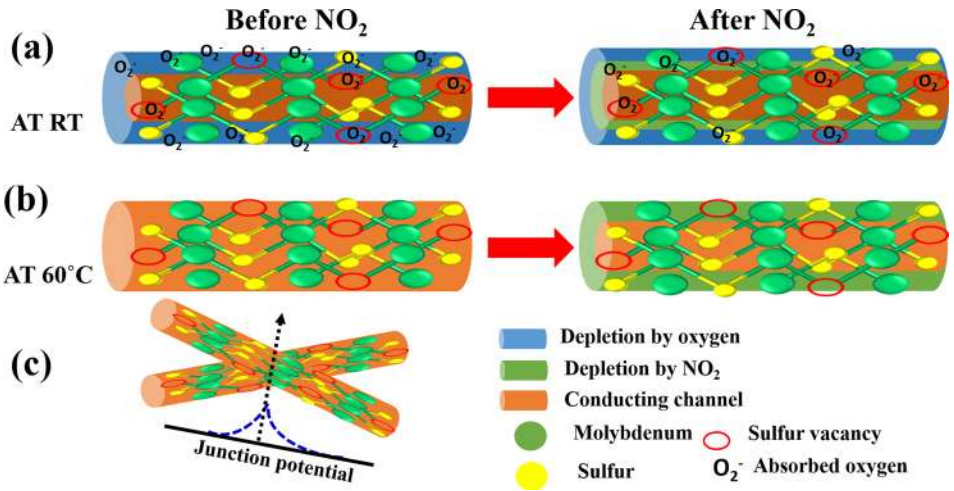

FIG. 5. Proposed sensing mechanism of the sensor: (a) at RT (more depletion of electrons by oxygen and humidity) and (b) at 60 °C (available abundant active sites to interact with NO_2 molecules). (c) Potential barrier formed at the intersection of the nanowires.

See supplementary material for I-V characteristic of the device in air and at 60 °C in a vacuum, resistance vs time graph of H_2S, CO_2, CH_4, and H_2 at optimum operating temperature (60 °C) of the sensor, and a comparison of this sensor with other previously reported NO_2 sensors in a tabular form.

The authors acknowledge the financial support of the Department of Science and Engineering Research Board (SERB) Project No. SERB/F/2236/2015-16 dated 16/07/2015.

[1]Environmental Protection Agency (EPA), www.epa.gov/air/nitrogenoxides/ for "Air Pollution, 2013" (last accessed June 06, 2013).
[2]R. Kumar, N. Goel, and M. Kumar, ACS Sens. **2**(11), 1744 (2017).
[3]V. A. Agrawal, R. Kumar, S. Venkatesan, A. Zakhidov, Z. Zhu, J. Bao, M. Kumar, and M. Kumar, Appl. Phys. Lett. **111**, 093102 (2017).
[4]S. Y. Cho, S. J. Kim, Y. Lee, J. S. Kim, W. B. Jung, H. W. Yoo, J. Kim, and H. Jung, ACS Nano **9**, 9314 (2015).
[5]D. J. Late, Y. K. Huang, B. Liu, J. Acharya, S. N. Shirodkar, J. Luo, A. Yan, D. Charles, U. V. Waghmare, V. P. Dravid, and C. N. R. Rao, ACS Nano **7**, 4879 (2013).
[6]K. F. Mak, C. Lee, J. Hone, J. Shan, and T. F. Heinz, Phys. Rev. Lett. **105**, 136805 (2010).
[7]S. Fathipour, M. Remskar, A. Varlec, A. Ajoy, R. Yan, S. Vishwanath, S. Rouvimov, W. S. Hwang, H. G. Xing, D. Jena, and A. Seabaugh, Appl. Phys. Lett. **106**, 022114 (2015).
[8]H. Xu, S. Liu, Z. Ding, S. J. R. Tan, K. M. Yam, Y. Bao, C. Tai Nai, M.-F. Ng, J. Lu, C. Zhang, and K. P. Loh, Nat. Commun. **7**, 12904 (2016).
[9]J. Kibsgaard, A. Tuxen, M. Levisen, E. Lægsgaard, S. Gemming, G. Seifert, J. V. Lauritsen, and F. Besenbacher, Nano Lett. **8**, 3928 (2008).
[10]T. Wang, D. Huang, Z. Yang, S. Xu, G. He, X. Li, N. Hu, G. Yin, D. He, and L. Zhang, Nano-Micro Lett. **8**(2), 95 (2016).
[11]H. Kadhim, H. A. Hassan, and Q. N. Abdullah, Nano-Micro Lett. **8**(1), 20 (2016).
[12]A. Saaedi and R. Yousefi, J. Appl. Phys. **122**, 224505 (2017).
[13]D. Liu, L. Lin, Q. Chen, H. Zhou, and J. Wu, ACS Sens. **2**, 1491 (2017).
[14]S. J. Kim, J.-W. Han, B. Kim, and M. Meyyappan, ACS Sens. **2**, 1679 (2017).
[15]Y. Feldman, E. Wasserman, D. J. Srolovitz, and R. Tenne, Science **267**, 222–225 (1995).
[16]S. Han, C. Yuan, X. Luo, Y. Cao, T. Yu, Y. Yang, Q. Li, and S. Ye, RSC Adv. **5**, 68283 (2015).
[17]B. Lei, G. R. Li, and X. P. Gao, J. Mater. Chem. A **2**, 3919 (2014).
[18]C. Lee, H. Yan, L. E. Brus, T. F. Heinz, J. Hone, and S. Ryu, ACS Nano **4**, 2695 (2010).
[19]S. M. Tan, A. Ambrosi, Z. Sofer, S. Huber, D. Sedmidubsky, and M. Pumera, Chem. Eur. J. **21**, 7170 (2015).
[20]G. R. Bhimanapati, T. Hankins, Y. Lei, R. A. Vila, I. Fuller, M. Terrones, and J. A. Robinson, ACS Appl. Mater. Interfaces **8**, 22190 (2016).
[21]B. Cho, M. G. Hahm, M. Choi, J. Yoon, A. R. Kim, Y.-J. Lee, S.-G. Park, J.-D. Kwon, C. Su Kim, M. Song, Y. Jeong, K. S. Nam, S. Lee, T. J. Yoo, C. G. Kang, B. H. Lee, H. Cho Ko, P. M. Ajayan, and D.-H. Kim, Sci. Rep. **5**, 8052 (2015).
[22]L. A. Currie, Pure Appl. Chem. **67**, 1699 (1995).
[23]Q. Yue, Z. Shao, S. Chang, and J. Li, Nano. Res. Lett. **8**, 425 (2013).
[24]S. Zhao, J. Xue, and W. Kang, Chem. Phys. Lett. **595**, 35 (2014).
[25]H. Qiu, L. Pan, Z. Yao, J. Li, Y. Shi, and X. Wang, Appl. Phys. Lett. **100**, 123104 (2012).
[26]W. Park, J. Park, J. Jang, H. Lee, H. Jeong, K. Cho, S. Hong, and T. Lee, Nanotechnology **24**, 095202 (2013).
[27]G. Li, D. Zhang, Q. Qiao, Y. Yu, D. Peterson, A. Zafar, R. Kumar, S. Curtarolo, F. Hunte, S. Shannon, Y. Zhu, W. Yang, and L. Cao, J. Am. Chem. Soc. **138**, 16632 (2016).
[28]M. V. Bollinger, J. V. Lauritsen, K. W. Jacobsen, J. K. Nørskov, S. Helveg, and F. Besenbacher, Phys. Rev. Lett. **87**, 196803 (2001).
[29]C. Ataca, H. Sahin, E. Akturk, and S. Ciraci, J. Phys. Chem. C **115**, 3934 (2011).